Title

Diagnosis of subglottic stenosis in a rabbit model using long-range optical coherence tomography

Journal

The Laryngoscope, 127(1)

ISSN

0023-852X

Authors

Ajose-Popoola, Olubunmi

Su, Erica

Hamamoto, Ashley

et al.

Publication Date

2017

DOI

10.1002/lary.26241

Peer reviewed

HHS Public Access

Author manuscript

Laryngoscope. Author manuscript; available in PMC 2018 January 01.

Published in final edited form as:

Laryngoscope. 2017 January ; 127(1): 64–69. doi:10.1002/lary.26241.

Diagnosis of Subglottic Stenosis in a Rabbit Model Using Long-Range Optical Coherence Tomography

Olubunmi Ajose-Popoola, MD[1,*], **Erica Su, BS**[2,*], **Ashley Hamamoto, BS**[2], **Alex Wang, BS**[2], **Joseph C. Jing, PhD**[2,3], **Tony D. Nguyen, BS**[2,4], **Jason J. Chen, BS**[2], **Kathryn E. Osann, PhD**[4], **Zhongping Chen, PhD**[2,3], **Gurpreet S. Ahuja, MD**[1,5], and **Brian J.F. Wong, MD, PhD**[1,2,3]

[1]Department of Otolaryngology—Head and Neck Surgery, University of California Irvine

[2]Beckman Laser Institute, University of California Irvine

[3]Department of Biomedical Engineering, University of California Irvine

[4]School of Medicine, University of California Irvine

[5]CHOC Children's Hospital of Orange County

Abstract

Objective—Current imaging modalities lack the necessary resolution to diagnose subglottic stenosis. The aim of this study is to use optical coherence tomography (OCT) to evaluate nascent subglottic mucosal injury and characterize mucosal thickness and structural changes using texture analysis in a simulated intubation rabbit model.

Study Design—Prospective animal study in rabbits.

Methods—Three-centimeter-long sections of endotracheal tubes (ETT) were endoscopically placed in the subglottis and proximal trachea of New Zealand white rabbits (n=10) and secured via suture. OCT imaging and conventional endoscopic video was performed just prior to ETT segment placement (Day 0), immediately after tube removal (Day 7), and one week later (Day 14). OCT images were analyzed for airway wall thickness and textural properties.

Results—Endoscopy and histology of intubated rabbits showed a range of normal to edematous tissue, which correlated with OCT images. The mean airway mucosal wall thickness measured using OCT was 336.4μm (Day 0), 391.3μm (Day 7), and 420.4μm (Day 14) with significant differences between Day 0 and Day 14 ($p=0.002$). Significance was found for correlation and homogeneity texture features across all time points ($p<0.05$).

Correspondence and request for reprints: Brian J-F. Wong, MD, PhD, Professor and Vice Chairman, Dept. of Otolaryngology-Head & Neck Surgery University of California Irvine, 1002 Health Sciences Road, Irvine, CA 92617, bjwong@uci.edu, Phone number: 949-824-4770, Fax number: 949-824-8413.

*These authors contributed equally to the study

Level of Evidence: NA

Presented at SPIE Photonics West, San Francisco, CA, USA on February 13, 2016.

Conflict of Interest and Financial Disclosures

Dr. Zhongping Chen has a financial interest in OCT Medical Imaging, Inc., which, however, did not provide support for this work.

Conclusion—OCT is a minimally invasive endoscopic imaging modality capable of monitoring progression of subglottic mucosal injury. This study is the first to evaluate mucosal injury during simulated intubation using serial OCT imaging and texture analysis. OCT and texture analysis have the potential for early detection of subglottic mucosal injury, which could lead to better management of the neonatal airway and limit the progression to stenosis.

Keywords

subglottic stenosis; optical coherence tomography; rabbit model; diagnostic imaging; intubation injury

Introduction

Acquired subglottic stenosis (SGS) is most commonly caused by prolonged intubation or intubation with an oversized endotracheal tube (ETT). Mucosal injury, as a result of ischemic necrosis, typically occurs at the subglottis because the cricoid cartilage is a continuous ring, which does not flex with pressure or allow centrifugal displacement of inflammatory edema. Ulceration of the subglottic epithelium may occur within hours of intubation and permanent damage is frequently observed within the first 7 days. Although the incidence of neonatal acquired SGS is approximately 0.24–2.0%, the development of SGS may have devastating consequences[1].

Early diagnosis of SGS is not possible using imaging modalities such as CT and MRI as they lack the necessary imaging resolution. SGS is managed with a range of surgical and endoscopic procedures[2]; however, these procedures may lead to re-stenosis due to induced inflammation, requiring additional anti-inflammatory treatments[3]. Direct laryngoscopy and bronchoscopy with dilation is the gold standard for the management of SGS, but it presents with the operative risks of losing a stable, intubated airway and hypoxia. Consequently, the treatment of neonatal SGS remains a diagnostic challenge for otolaryngologists.

There have been several SGS models in rabbits using direct trauma to the mucosa (i.e., brushing, caustic chemicals) but very few in evaluating the use of imaging modalities on ETT injury[4]. Optical coherence tomography (OCT) is an emerging minimally invasive optical imaging technique that provides high resolution (~10 μm) images of living tissue based on different optical properties. OCT has profound impact in diagnosis and management of retinal disease in ophthalmology, and has been evaluated intensely in coronary vasculature and GI tract imaging[5,6]. Traditionally, OCT has focused primarily on imaging the upper aerodigestive tract and vocal fold diseases[7–9]. Our group, along with others, have also focused on the developing pediatric airway as a new application for OCT[10–12].

Texture analysis is an objective and automated method to obtain quantifiable information from medical images for the purposes of tissue classification, lesion detection, and pathologic quantification[13]. In a digital image, texture is defined as the spatial distribution of intensity values, while texture analysis is the evaluation of the relative position and intensity of these pixels[13]. Texture properties derived from gray-level co-occurrence matrices (GLCM)—a commonly used statistical approach—have been investigated to characterize

tissues imaged with OCT[14]. The main properties successfully used to objectively classify tissue include contrast, correlation, homogeneity, and energy[14,15]. As OCT studies generate hundreds to thousands of images per patient, automated or semi-automated analysis is essential, particularly if this technology evolves into a screening measure in the neonatal intensive care unit (NICU).

The study objectives are to evaluate OCT as an imaging modality to 1) detect nascent subglottic injury from simulated prolonged intubation in a rabbit model, 2) obtain measurements of airway wall morphology, and 3) perform automated texture analysis for diagnosis of the condition.

Methods

OCT System

The details of the OCT device and instrumentation used in this study are available in the online supplement and have been previously described[16]. The flexible OCT probes were custom-built with outer diameters of 1.2 mm and placed within a fluorinated ethylene propylene sheath (Zeus Inc., Orangeburg, SC). The probes were then rotated proximally while being retracted, acquiring images in a retrograde, helical fashion. The system has an axial and a lateral resolution of approximately 10 μm and 112 μm, respectively.

Rabbit Model and Data Acquisition

Ethical approval for this study was obtained from the University of California Institutional Animal Care and Use Committee. Ten New Zealand white rabbits (2.4–4.3 kg) were used. At this weight and stage of development, the airway dimensions at the level of the cricoid (5.4–5.8 mm) approximate that of neonates (4.5–5.5 mm)[17].

The intubation-induced subglottic injury model developed by Kelly et al. was adapted for this study[4]. A detailed description of the surgical technique and procedure is available in the online supplement. On Day 0, a 3-cm long section of ETT was endoscopically placed just below the vocal cords (subglottis and proximal trachea) and secured with a suture via a small cervical incision. Prior to insertion, the subglottis was sized with an appropriately tight fitting ETT (3.5–4.0). OCT and digital video imaging was conducted prior to ETT placement from 3 cm below the subglottis to the level of the glottis. On Day 7, imaging was acquired after the segment of ETT was endoscopically removed. On Day 14, the animal was euthanized after imaging. The larynx and proximal trachea were dissected free and fixed in formaldehyde for 24 hours. The samples were then processed, embedded in paraffin, and sequentially sectioned into 6 μm thick slices for histological analysis (hematoxylin-eosin staining).

Data Analysis

Histologic sections of the subglottis were examined using light microscopy (Microphot-FXA; Nikon) and digitized (PictureFrame; Optronics) for documentation. The mucosal and submucosal layers of the specimen were visually compared to the control specimen from a

parallel study for changes in thickness and mucosal lining. The sections were also compared to corresponding OCT images.

Morphometric and texture analyses were performed on the subglottic region. The tissue segmentation and micrometry methods have been previously described[18]. Figure 1A shows a representative linear image (Figure 1A) and Figure 1B shows a circular image (analogous to CT axial images) of the subglottis with manual segmentation in Figure 1C–D. The statistical values (i.e., mean, standard deviation, and range) of the thickness were calculated across all axial-lines of the segmented region of each animal. The average statistical values of each experimental day is reported in Table E1.

Texture analysis was performed on the segmented images. Sixteen texture features (contrast, correlation, energy, and homogeneity) were derived from GLCM (0°, 45°, 90°, and 135°) per image. The mean values per experimental day and their standard error were reported. The repeated measures analysis of variance (rANOVA) was used to measure changes across the 3 time points. Pairwise differences were performed using a one-tailed Student t-test with Bonferroni correction to adjust for the multiple comparisons.

Results

Morbidity and Mortality

Two out of 10 rabbits were excluded from the study: one died as a consequence of a witnessed aspiration during the intubation process, and the other was excluded after one week of intubation as the ETT segment was found to have migrated to the distal trachea.

Endoscopic and Histologic Analyses

Preintubation endoscopy of all animal subjects was confirmed to be negative for injury in the subglottis prior to the surgical procedure. Control endoscopy of the subglottis was taken to allow subsequent comparison (Figure 2A). ETT and suture placement was verified endoscopically (Figure 2B). Following extubation, endoscopy of the animal subjects uniformly demonstrated edema and inflammation (Figure 2C). Five of the 8 animals demonstrated focal areas of ulceration by Day 14 of the study (Figure 2D).

Histologic sections at the level of the cricoid were compared between the intubated group at Day 14 and controls from a parallel study[19]; no animals were euthanized on Day 7. In the intubated animals, there was evidence of mucosal thickening in both the epithelium and underlying lamina propria (Figure 3). Regions of the mucosal layer demonstrated signs of epithelial metaplasia and abnormal basement membranes with the presence of inflammatory cells. In the submucosa, there was indication of increased vascularity and development of granulation tissue.

OCT Analysis: Soft Tissue Thickness and Texture Analysis

Images of Day 0 (control) demonstrated subglottic epithelial layer of low intensity pixels while the underlying lamina propria presented a uniform layer of higher intensity (Figure 4A). Darker regions within the submucosal layer indicated the presence of submucosal glands or blood vessels, and the first tracheal ring and perichondrium were clearly visible.

Images obtained on Day 7, following ETT segment removal, indicated significant pathology (Figure 4B). The contrast between the substructures was less pronounced, and the lamina propria and submucosa were darker and degraded in appearance. This observation is consistent with granulation tissue and edema[10], which were also observed with conventional digital endoscopy. The subglottic airway also demonstrated circumferential narrowing. Images obtained on Day 14 showed marked thickening of the mucosa and submucosa (Figure 4C). The contrast between the mucosal substructures was comparable to the control and visibly different from images obtained on Day 7; however, the contour of the subglottis was more irregular and focal regions of ulceration were observed.

Segmentation of the airway cross-section divided the axial tissue structures into 1) the airspace, 2) the mucosa and the submucosa, and 3) the cartilage layer. The mean thickness of the mucosa and submucosa layer was 336.4 ± 20.7 μm on Day 0, 391.3 ± 22.9 μm on Day 7, and 420.4 ± 15.4 μm on Day 14. There was a significant increase in thickness between Day 0 and Day 14 of imaging ($p=0.002$). Between Day 0 and Day 7, the increase was nearly significant ($p=0.053$). Figure 5 shows a graphical representation of the mean thickness measurements for each animal across the 3 imaging days with standard error of the means.

Analysis with rANOVA showed statistically significant increases for correlation and homogeneity variables for all directions across the 3 time points ($p<0.05$). Running pairwise comparisons between the levels, there was significance between Day 0 and Day 14 for correlation in all directions ($p\leq0.016$). Changes between Day 0 and Day 7 did not reach statistical significance ($p\geq0.06$ for all directions). For contrast, homogeneity, and energy parameters, there were noticeable trends in all directions across the 3 time points. Contrast values decreased between Day 0 and Day 7 and returned to values more similar to the control on Day 14. Energy and homogeneity values increased between Day 0 and Day 7 and returned to more similar values to the control on Day 14. Details of the statistical analysis are found in Table E1.

Discussion

In our previous study in critically ill intubated neonates in the NICU, OCT measurement of soft tissue changes in the subglottic mucosa was reported[20]. However, we were not able to correlate endoscopic images or histopathology, as the number of subjects progressing to operative endoscopy was small, and full thickness (including cartilage) surgical specimens are rarely available in these subjects[20]. In this study, the animal model was used to simulate the clinical scenario (intubation) to provide insight into the relationship between OCT, histologic, and endoscopic observations. Early injury due to prolonged intubation cannot be diagnosed using conventional imaging modalities (CT, MRI, etc.) due to their limited imaging resolution. Direct laryngoscopy is the gold standard of the diagnosis of SGS, but is generally performed under general anesthesia, which could result in complete airway obstruction. Alternatively, OCT can be performed daily as a screening measure through the endotracheal tube and would not require extubation or endoscopy. With its high resolution, OCT may detect early signs of SGS, providing a means to better manage the ETT, prevent progression to high-grade SGS, and even predict patients with high risk for extubation failure.

This study illustrates the potential for OCT to detect mucosal injury and thickening in the subglottis. Soft tissue layer thickness measurements and texture analysis demonstrated statistically significant increases in mucosal and submucosal thickness and changes in texture parameters over time, respectively. The model used here best replicates the clinical circumstances, where the ETT remains in the airway for a prolonged time period. Texture analysis has been used in many settings particularly in remote sensing and machine vision applications[21]. Here, texture analysis is demonstrated as an automated means to analyze tissue.

Previous SGS models with arduous methods (i.e., electrocautery, chemical irritation, curette, laser, nylon brush) produced high-grade stenoses associated with high mortality rates and did not mimic clinical neonatal SGS[19,22–25]. Actual intubation models have been used, however only acute changes can be studied due to limitations with respect to how long a rabbit can remain intubated[26]. In contrast, the ETT model developed by Kelly et al. has demonstrated to increase lamina propria thickness, mucosal thickness, and goblet cell density[4]. The mucosal injuries induced in this study were similar, though no perichondritis or chondritis was observed. This is possibly due to differences in ETT sizing, as the degree of injury depends on the pressure induced by the oversized ETT. Regardless, ulceration, granulation tissue, and mucosal thickening were observed. The superficial injury created here is more similar to what is believed to occur during the early stages of subglottic injury in the neonate, which is seldom clinically documented as operative endoscopy is rarely, if ever, performed at this time in disease evolution. Additionally, OCT tracked mucosal thickening over 3 time points in the same animal, while other animal studies have relied entirely upon histology obtained only at euthanasia.

A limiting factor in this study was not including micrometry of histologic sections at different time points as histology is only available on Day 14, the time in which euthanasia occurred. Animal subject numbers were kept limited because previous studies have already demonstrated the link between OCT-based measurements of mucosal thickness and histology[19]. Furthermore, micrometry based upon histologic sections is fraught with artifact due to fixation methods, whereas OCT micrometry is precise to less than 10 μm[27].

Mucosal thickness was found to increase through one week of intubation and continued to increase after extubation. There was statistical significance between measurements on Day 0 and Day 14, near significance between Day 0 and Day 7, and no significance between Day 7 and 14. This suggests that most of the mucosal injury occurs within the week of intubation while the inflammatory process may have continued even after extubation. These findings correlate with the signs of early SGS, including ischemia and edema caused by prolonged mucosal compression, then ulceration, inflammation, and granulation tissue formation following persistent injury. After extubation, the healing of subglottic ulcers continues and follows a similar pathway as wound healing of the skin[28].

Each OCT scan includes hundreds of images, and if used as a clinical screening measure, automated or semi-automated processes may be required. In this study, labor intensive manual segmentation of distinct tissue regions was performed by one investigator (E.S.). The feasibility of texture analysis using OCT images for the purposes of tissue classification

have been reported, though use has not been widespread[14,29]. GLCM properties potentially allow differentiation of tissue type without manual segmentation[14] and of tissue phantoms containing various sizes and distributions of scattering foci[29]. To our knowledge, our investigation is the first to apply texture analysis to airway OCT images. Changes in the texture statistics show measurable differences between pathological states of the intubated subglottis. The significant changes in correlation and homogeneity herein demonstrate potential for automated diagnosis. In addition, the trends in homogeneity and energy indicate an increase in the value after one week of intubation followed by a return to values similar to the control after one week following extubation. Contrast showed a decrease followed by a return to values similar to the control.

Conclusion

This study is the first to characterize ETT injury to the rabbit airway using OCT and apply texture analysis to detect changes in tissue composition. OCT allows for quantifiable measurements of airway soft tissue thickening, showing statistically significant changes across different time points. Texture analysis provides a basis to characterize the state of the pathology relative to the control, and the success herein makes automated classification of pathology possible. Such an automated approach would be essential should OCT evolve to become a common part of ETT and airway management in the NICU. Future studies will focus on combining this ETT SGS injury model with pepsin and hydrochloric acid application to simulate acid reflux.

Supplementary Material

Refer to Web version on PubMed Central for supplementary material.

Acknowledgments

This study was supported by National Institutes of Health (NIH) award numbers: 1-R01-HL103764-01 and 1-R01-HL105215-01 from the National Heart, Lung and Blood Institute (NHLBI), 1-R43-HD071701-01 from the National Institute of Child Health and Human Development (NICHD), and P41EB015890 from the National Institute of Biomedical Imaging and Bioengineering (NIBIB).

References

1. Walner DL, Loewen MS, Kimura RE. Neonatal Subglottic Stenosis-Incidence and Trends. Laryngoscope. 2001; 111(1):48–51. DOI: 10.1097/00005537-200101000-00009 [PubMed: 11192899]
2. Wei JL, Bond J. Management and prevention of endotracheal intubation injury in neonates. Curr Opin Otolaryngol Head Neck Surg. 2011; 19(6):474–477. DOI: 10.1097/MOO.0b013e32834c7b5c [PubMed: 21986802]
3. Ingrams DR, Ashton P, Shah R, Dhingra J, Shapshay SM. Slow-release 5-fluorouracil and triamcinolone reduces subglottic stenosis in a rabbit model. Ann Otol Rhinol Laryngol. 2000; 109(4):422–424. [PubMed: 10778898]
4. Kelly NA, Murphy M, Giles S, Russell JD. Subglottic injury: A clinically relevant animal model. Laryngoscope. 2012; 122(11):2574–2581. DOI: 10.1002/lary.23515 [PubMed: 22961393]
5. Gerckens U, Buellesfeld L, McNamara E, Grube E. Optical coherence tomography (OCT): Potential of a new high-resolution intracoronary imaging technique. Herz. 2003; 28(6):496–500. DOI: 10.1007/s00059-003-2485-9 [PubMed: 14569390]

6. Costa RA, Skaf M, Melo LAS, et al. Retinal assessment using optical coherence tomography. Prog Retin Eye Res. 2006; 25(3):325–353. DOI: 10.1016/j.preteyeres.2006.03.001 [PubMed: 16716639]
7. Sepehr A, Armstrong WB, Guo S, et al. Optical coherence tomography of the larynx in the awake patient. Otolaryngol - Head Neck Surg. 2008; 138(4):425–429. DOI: 10.1016/j.otohns.2007.12.005 [PubMed: 18359348]
8. Kobler JB, Chang EW, Zeitels SM, Yun SH. Dynamic imaging of vocal fold oscillation with four-dimensional optical coherence tomography. Laryngoscope. 2010; 120(7):1354–1362. DOI: 10.1002/lary.20938 [PubMed: 20564724]
9. Ridgway JM, Armstrong WB, Guo S, et al. In vivo optical coherence tomography of the human oral cavity and oropharynx. Arch Otolaryngol Head Neck Surg. 2006; 132(10):1074–1081. DOI: 10.1001/archotol.132.10.1074 [PubMed: 17043254]
10. Ridgway JM, Ahuja G, Guo S, et al. Imaging of the Pediatric Airway Using Optical Coherence Tomography. 2007; 117doi: 10.1097/MLG.0b013e318145b306
11. Lazarow FB, Ahuja GS, Chin Loy A, et al. Intraoperative long range optical coherence tomography as a novel method of imaging the pediatric upper airway before and after adenotonsillectomy. Int J Pediatr Otorhinolaryngol. 2015; 79(1):63–70. DOI: 10.1016/j.ijporl.2014.11.009 [PubMed: 25479699]
12. Volgger V, Sharma GK, Jing JC, et al. Long-range Fourier domain optical coherence tomography of the pediatric subglottis. Int J Pediatr Otorhinolaryngol. 2015; 79(2):119–126. DOI: 10.1016/j.ijporl.2014.11.019 [PubMed: 25532671]
13. Castellano G, Bonilha L, Li LM, Cendes F. Texture analysis of medical images. Clin Radiol. 2004; 59:1061–1069. DOI: 10.1016/j.crad.2004.07.008 [PubMed: 15556588]
14. Gossage KW, Tkaczyk TS, Rodriguez JJ, Barton JK. Texture analysis of optical coherence tomography images: feasibility for tissue classification. J Biomed Opt. 2003; 8(3):570–575. DOI: 10.1117/1.1577575 [PubMed: 12880366]
15. Lin Y-S, Chu C-C, Lin J-J, et al. Optical coherence tomography: A new strategy to image planarian regeneration. Sci Rep. 2014; 4:6316.doi: 10.1038/srep06316 [PubMed: 25204535]
16. Jing J, Zhang J, Loy AC, Wong BJF, Chen Z. High-speed upper-airway imaging using full-range optical coherence tomography. J Biomed Opt. 2012; 17(11):110507.doi: 10.1117/1.JBO.17.11.110507 [PubMed: 23214170]
17. Loewen MS, Walner DL. Dimensions of rabbit subglottis and trachea. Lab Anim. 2001; 35(3):253–256. DOI: 10.1258/0023677011911714 [PubMed: 11459410]
18. Su, E., Sharma, GK., Chen, J., et al. Analysis and digital 3D modeling of long-range fourier-domain optical coherence tomography images of the pediatric subglottis. In: Choi, B.Kollias, N.Zeng, H., et al., editors. Proc. SPIE 8926, Photonic Therapeutics and Diagnostics X; 2014. p. 89262J
19. Lin JL, Yau AY, Boyd J, et al. Real-Time Subglottic Stenosis Imaging Using Optical Coherence Tomography in the Rabbit. JAMA Otolaryngol Neck Surg. 2013; 139(5):502.doi: 10.1001/jamaoto.2013.2643
20. Sharma GK, Ahuja GS, Wiedmann M, et al. Long Range Optical Coherence Tomography of the Neonatal Upper Airway for Early Diagnosis of Intubation-related Subglottic Injury. Am J Respir Crit Care Med. Jul.2015 150727130422005. doi: 10.1164/rccm.201501-0053OC
21. du Buf JMH, Kardan M, Spann M. Texture feature performance for image segmentation. Pattern Recognit. 1990; 23(3–4):291–309. DOI: 10.1016/0031-3203(90)90017-F
22. Cincik H, Gungor A, Cakmak A, et al. The effects of mitomycin C and 5-fluorouracil/triamcinolone on fibrosis/scar tissue formation secondary to subglottic trauma (experimental study). Am J Otolaryngol. 2005; 26(1):45–50. [PubMed: 15635581]
23. Roh JL, Lee YW, Park HT. Subglottic wound healing in a new rabbit model of acquired subglottic stenosis. Ann Otol Rhinol Laryngol. 2006; 115(8):611–616. [PubMed: 16944660]
24. Steehler MK, Hesham HN, Wycherly BJ, Burke KM, Malekzadeh S. Induction of tracheal stenosis in a rabbit model-endoscopic versus open technique. Laryngoscope. 2011; 121(3):509–514. DOI: 10.1002/lary.21407 [PubMed: 21344426]

25. Chafin JB, Sandulache VC, Dunklebarger JL, et al. Graded carbon dioxide laser-induced subglottic injury in the rabbit model. Arch Otolaryngol Head Neck Surg. 2007; 133(4):358–364. DOI: 10.1001/archotol.133.4.358 [PubMed: 17438250]

26. Kumar SP, Ravikumar A, Thanka J. An animal model for laryngotracheal injuries: An experimental study. Laryngoscope. 2015; 125(1):E23–E27. DOI: 10.1002/lary.24867 [PubMed: 25111795]

27. Kaiser ML, Rubinstein M, Vokes DE, et al. Laryngeal epithelial thickness: A comparison between optical coherence tomography and histology. Clin Otolaryngol. 2009; 34(5):460–466. DOI: 10.1111/j.1749-4486.2009.02005.x [PubMed: 19793279]

28. Eid, Ea. Anesthesia for subglottic stenosis in pediatrics. Saudi J Anaesth. 2009; 3(2):77–82. DOI: 10.4103/1658-354X.57882 [PubMed: 20532108]

29. Gossage KW, Smith CM, Kanter EM, et al. Texture analysis of speckle in optical coherence tomography images of tissue phantoms. Phys Med Biol. 2006; 51(6):1563–1575. DOI: 10.1088/0031-9155/51/6/014 [PubMed: 16510963]

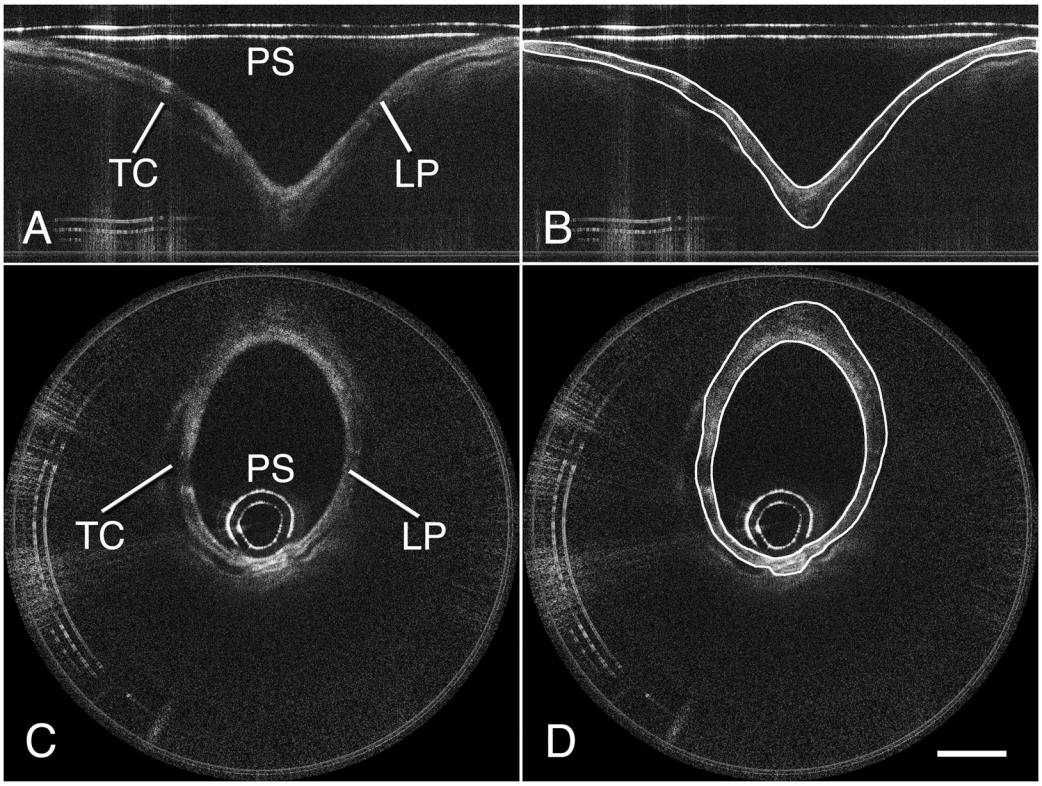

Figure 1.

Representative OCT image of the rabbit subglottis in linear (A) and circular representation (C). Sample segmented images in linear (B) and circular representation (D). Scale bar represents 2 mm. Definition of abbreviations: TC = tracheal cartilage, LP = lamina propria, PS = outer probe sheath.

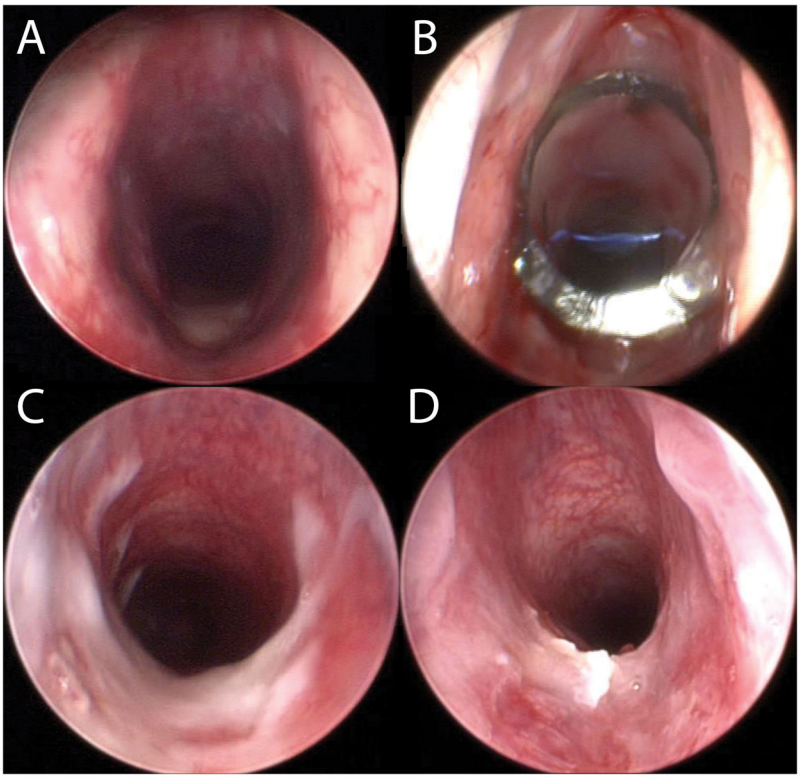

Figure 2.

Endoscopic footage of gross morphology of the subglottis. (A) The control subglottic region and (B) subglottic region after tube placement with clear visualization of the suture. (C) Edema and inflammation apparent after one week of intubation and (D) focal areas of ulceration after one week of extubation.

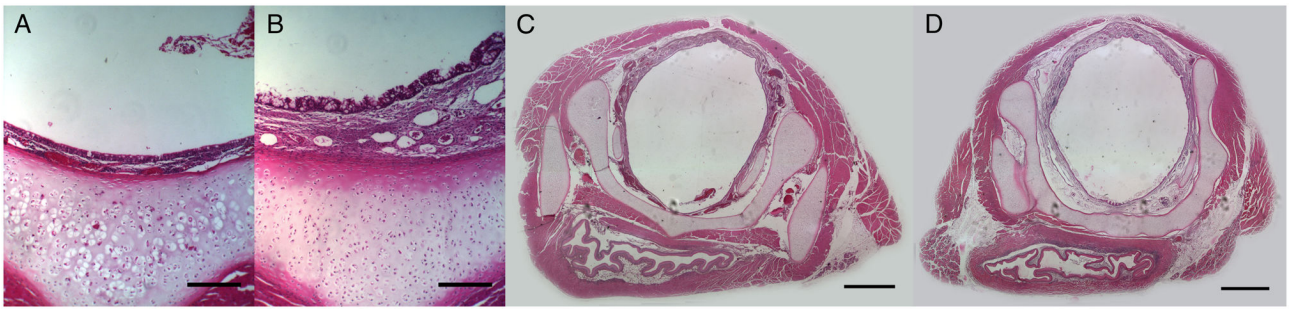

Figure 3.

Histologic comparison between control and intubated specimen. (A) The normal mucosal and submucosal layers of an unintubated animal and (B) thickened mucosal and submucosal layers of an intubated animal sacrificed after one week of extubation. Scale bars for (A) and (B) represent 250 μm. (C) Entire section of the normal subglottis at the level of the cricoid cartilage. (D) Entire section of the intubated subglottis with evidence of edema and granulation tissue. Scale bars for (C) and (D) represent 2 mm.

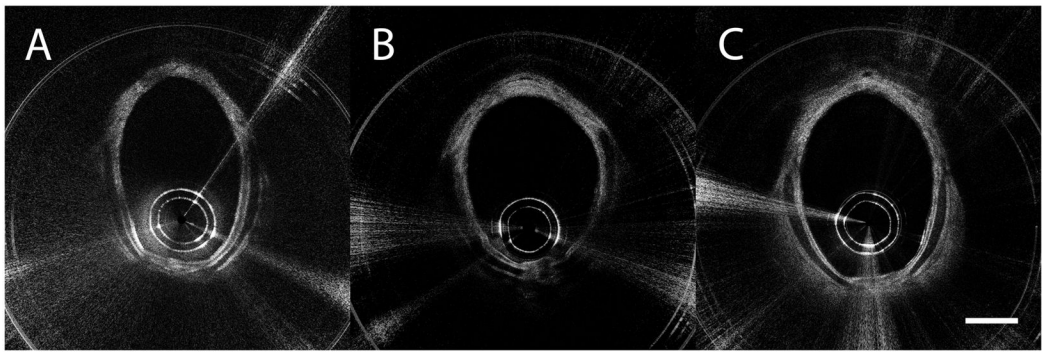

Figure 4.

OCT images of the subglottis at different time points. (A) Control subglottic region showing normal anatomy. (B) Thickened mucosal layer of the subglottic region with evidence of edema (darker regions) after one week of intubation. (C) Thickened mucosal and submucosal layers after one week of extubation. Scale bar represents 2 mm.

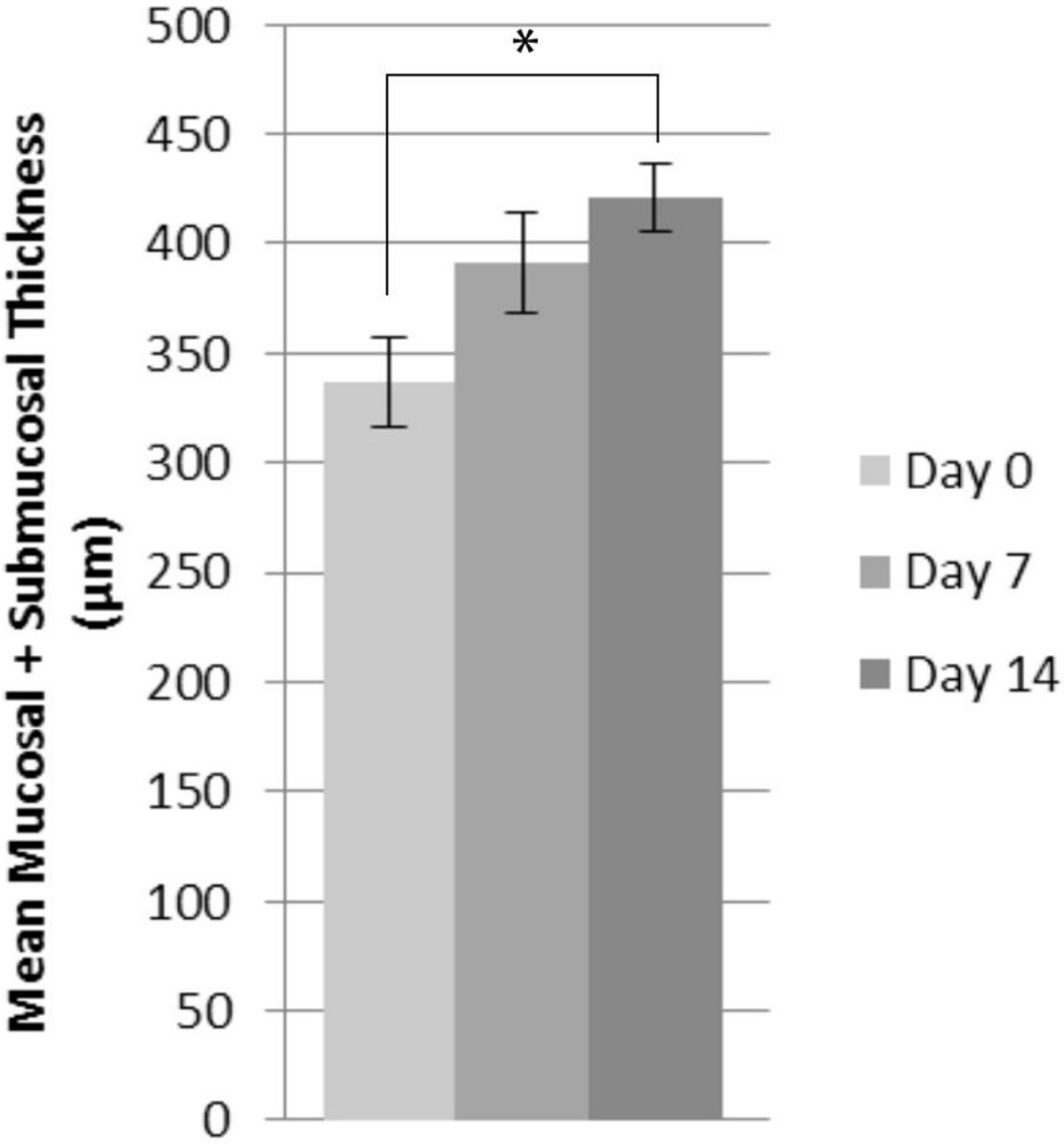

Figure 5.
Graphical representation of the effect of intubation on the mucosal and submucosal thickness. Mean airway soft tissue thickness measurements of all animals are shown with significant increase in thickness between Day 0 and Day 14 (*p = 0.002).